Lime mud waste from the paper industry as a partial replacement of cement in mortars used on radiant floor heating systems

R. Borinaga- Treviño [*], J. Cuadrado, J. Canales, E. Rojí

Department of Mechanical Engineering, University of the Basque Country UPV/EHU, Bilbao, Spain

ARTICLE INFO

ABSTRACT

In order to mitigate climate change, reductions of energy consumption are required on heating systems for residential and non-residential buildings. Despite radiant floor heating systems are being widely used due to their high thermal efficiency and comfort, further improvements are necessary to reduce the carbon footprint of the mortars used. This paper studies the use of lime mud, a by-product of the paper industry, as a partial replacement of cement to reduce the environmental impact of the resulting mortar. For that purpose, a reference cement mortar is compared to mortars with 10%, 20%, 30% and 40% of cement replacement by weight. Physical, thermal and mechanical properties showed that up to 20% of cement could be replaced by lime mud while maintaining thermal properties of the mortar. Despite the reduction of the mechanical resistance, mortars with up to 20% of cement replacement fulfilled the requirements of EN 1264-4:2010 standard. Finally, tests on laboratory-made radiant floor heating slabs proved that slabs with reference mortar had a similar stationary behaviour to that of the slabs with mortar containing 20% of lime mud, but the latter reach stationary faster due to the lower thermal inertia of its mortar.

1. Introduction

Nowadays, radiant floor heating and cooling systems are being widely used in residential and non-residential buildings. There is a vast bibliography with the use of those systems. In South Korea, most of the residential buildings install those systems combined with ventilation systems [1]; in northern China, 85% of rural residential buildings had it also installed [2]; in central Europe the percentage is lower, 30%–50%, but a significant increase is also expected due to the climate change concern [3,4]. Radiant floor heating systems have some advantages over other systems such as radiators, fan-coils, etc. that make them interesting for both refurbished and new buildings.

The main advantage over other heating systems is related to its position, the floor. As most of the floor could be used as a heat emitter, the emitting surface could be significantly bigger, which lowers the temperature required by radiant floor heating systems (30-40 °C), making them more energy efficient than wall radiators (70 °C) [5]. According to Sebarchievici [6], the operating costs of radiant floor heating systems are up to 10% lower to those of wall radiators. Furthermore, radiant floor heating system provides higher thermal comfort due to their more uniform temperature distribution over the entire floor and creates a vertical, thermal gradient on the habitable space that is optimal for

the human body [5]. Precisely, the vertical thermal gradient also makes this system even more efficient to other alternatives for heating high-roof spaces, where most of the heat tends to go to the unused higher part of the space due to natural convection [3,4,7,8]. In addition, as radiant floor heating system heats the air of the habitable space mainly by natural convection and radiation, the movement of the air is lower than the one required for a proper functioning of an air-based heating system such as fan-coils, making the radiant floor a better alternative when the air quality is a critical factor [7]. Besides, those systems are hidden under the floor, making the space usually occupied by radiators available for other uses, which are often placed under the windows in order not to compromise the interior design, reducing even more their thermal efficiency. Consequently, the use of radiant floor heating systems is increasing, due to the low operating temperatures required; enabling them to use them combined with high-energy efficient heat pumps based on renewable energy sources: solar thermal, geothermal, aerothermal, etc. [7].

In general, radiant floor heating systems consist on an insulation, a piping system, a mortar and the final surface desired by the customer in each case. One alternative would be to improve the lower insulation by lighter and more insulating materials, such as the aerogel proposed by Kosny et al. [9]. However, the mortar used plays a key role on the final

---

efficiency of the system. On the one hand, the higher the mortar mechanical properties, the thinner could be the mortar layer, decreasing the thermal gradient between the heating source (embedded piping system) and the radiating surface. This could be important on refurbishment interventions, due to the reduction of the available room height inherent to this kind of systems. However, it does not have to be a problem in new buildings, where the thickness of the radiant floor heating systems could be included during the design in order to maintain an adequate available height. On the other hand, the higher the thermal conductivity and the lower the volumetric heat capacity of the mortar, the lower it is the temperature gradient mentioned before and the sooner the system reaches stationary regime. Nevertheless, as radiant floors are thought to work mainly on stationary regime, adding phase change materials to increase the volumetric heat capacity of the mortar is also a promising alternative to reduce the operation cost of the installation [10].

Anyway, in order to ease their construction process, the consistency of the fresh mortar needs to be self-compacting to minimize the air entrapped inside that would dramatically reduce the heating efficiency of the system. However, when hardened, mechanical properties of the mortar must be sufficient to withstand the loads required by the space usage. Consequently, mortars tend to have higher quantities of water and cement than those used in masonry mortars or concretes. Cement, being the second more consumed material of the world after water [11], is an avid consumer of natural resources and energy, thus its use must be minimized [12]. Cement production plants alone are responsible of 5–7% of global CO2 emissions [13]. Therefore, reducing cement use is paramount in order to make mortars more sustainable.

In this way, there are several research lines focused on the reduction of the use of cement on mortars by replacing them with alternative, industrial and agricultural by-products [14,15]. Cement could be partially replaced by activated paper sludge [16], rice husk [17], rice straws [18], and so on, but an additional energy consumption is required in any case during their activation process. In particular, the use of wastes from the paper industry has been widely studied [19–24]. Ouyang et al. [19] activated the pozzolanic properties of kaolin by-products from the paper industry to study its optimal cement replacement ratio on mortars. Results were promising, as replacing 15% of cement, both flexural and compressive strengths were improved by up to 20%. Vegas et al. [25] analyzed the durability of ternary cements containing up to 10.5 wt% of thermally activated paper sludge, concluding that the durability to marine environment and to freeze/thaw cycles of the resulting concrete was better to that of the ordinary Portland cement concrete. Yan and S. and Sagoe-Crentsil [20] studied the influence of replacing up to 10% of the cement used in masonry mortars by the de-inking sludge created during the paper recycling process, after oven drying it at 110 °C for 48 h. According to their results, when fresh, flow of the masonry mortar was significantly reduced due to the high water absorption of the dried sludge. Regarding the hardened properties, mechanical properties were also lessened, but both absorption and shrinkage were improved. Azevedo et al. [21,23] studied the use of liquid and dried primary sludge from the paper industry as a cement replacement on mortars. In both cases, mortars were more fluid than the reference mortar when fresh. However, in spite of the reduction of the density observed, mortars had similar compressive and flexural strengths to those of the reference mortar. Accordingly, Malaiskiene et al. [26] studied the replacement of up to 15% by mass of cement by paper mill sludge oven-dried at low temperature (75 °C) on both cement hydration and hardened mechanical properties. They concluded that the hydration process was delayed, but long-term mechanical properties were similar to those of the control specimens. This paper aims to study the influence of using oven-dried primary sludge from the paper industry as a cement replacement in self-compacting mortars used for radiant-floor heating systems.

2. Materials and methods

2.1. Materials and specimen preparation

CEM II-B (L)/32.5R type cement was used in agreement with EN 197-1. This cement has the highest replacement proportion by weight allowed for any addition by the standard in force, 35%, which agrees with the main goal of this research, that is, to replace as much Portland clinker as possible. In this case, the addition is limestone filler and the resulting cement is valid for the use in foundation concretes and masonry mortars in general. The lime mud is a by-product of the local paper industry SMURFIT KAPPA NERVION, which has Radiata pine as raw material. Being its fibre longer than that of other species, this wood is utilised for Kraft papermaking, for making paper bags and sacks. Madrid et al. [22] made a deeper analysis of the same lime mud, studying its chemical composition (X-ray fluorescence spectroscopy), its mineralogical analysis (X-ray Diffraction analysis), its morphology (Scanning Electron Microscope) and its thermal behaviour (Thermogravimetry/Differential Scanning Calorimetry). Properties of the lime mud and the limestone aggregate are shown in Fig. 1 and the main characteristics of the lime mud are summarized in Table 1. Grain-size distribution
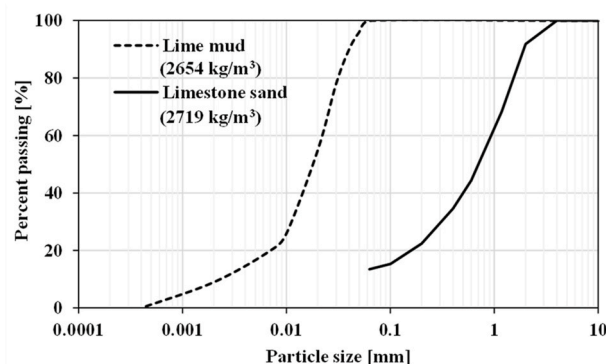

Fig. 1. Grain size distribution and apparent particle density of the aggregates.

Table 1
Summary of the lime mud properties reported by Madrid et al. [22].

Chemical composition, by X-ray Diffraction analysis (percentage by mass)											
SiO_2	Al_2O_3	Fe_2O_3	MnO	MgO	CaO	Na_2O	K_2O	TiO_2	P_2O_5	SO_3	LOI[a]
0.03	0.01	0.09	0.01	0.19	50.31	2.83	0.17	0.01	0.04	1.48	46.1

Content of C, H, N and S present in the by-products (percentage by mass)

C	H	N	S
13.11	<1	<1.6	<3

Morphology (Scanning Electron Microscope)
Lime mud contained few porous and many polyhedral shaped particles

X-Ray Diffraction analysis
Two crystalline phases are identified: Calcium Carbonate ($CaCO_3$) as the governing phase (>90%) and Portlandite ($Ca(OH)_2$) in small amounts (1–3%). No crystalline sulphur and sodium phases were detected.

Differential Scanning Calorimetry
- Minor endothermic peaks at temperatures below 125 °C, which is attributed to desorption and drying processes.
- An exothermic peak at 520 °C, and a strong endothermic peak at 828 °C; caused by calcite ($CaCO3$) decomposition.

Thermogravimetry

Temperature range [°C]	Total mass loss [%]	Cause
0-125 °C	3.069	Desorption and drying processes.
300-550 °C	4.939	Combustion of minor organic matter.
600–828 °C	43.239	Calcite decomposition

[a] Loss of ignition includes the water lost in the decomposition of small quantities of Portlandite detected in the XRD ($Ca(OH)_2$ consists of 79.7% CaO + 24.3% H_2O).

and apparent particle density (ρ_l) were determined according to EN 933-1 and EN 1097-6, respectively. CHRYSO 550 superplasticizer admixture was used as water reducer for obtaining self-compacting mortars.

Table 2 shows the mix proportions used in this research. All the mortars studied had the same binder (b):limestone sand (l) proportions by weight, 1:3. The difference between the mortars studied was on the binder. For the reference mortar (REF), cement was the only binder used, while on the other mixes, cement was partially replaced by calcium carbonate in four different proportions: 10%, 20%, 30% and 40% by weight, on C10, C20, C30 and C40 mortars, respectively. 1% of superplasticizer (sp) by unit weight of cement was used in any case, meaning that the higher the lime mud content used, the lower the sp content required on the mix.

Consistency of the fresh mortar was determined by the flow table test according to EN 1015-3 as it was done on previous releases [27–30]. Two different water to binder ratios were adjusted per each mortar studied with the aim of determining the sensitivity of the mixes to the water proportion used: 180–200 mm (subscript 1) and 220–240 mm (subscript 2). Mortars with the former consistency were pumpable, nearly self-compacting. In this case, the casting process would not require any specific equipment to spread the mix through the entire surface, but would require a slight superficial vibration and levelling during casting. This mortar represented the lowest water to binder ratio that would permit the confection of a mortar designed for radiant floor heating systems. The latter mortar was self-levelling, but its consistency was on the lower boundary for that purpose, in order to avoid unnecessary reductions of its mechanical and thermal properties. Mixing process was similar for all the batches according to the following sequence:

- Cement, calcium carbonate and limestone sand were dry-mixed (low speed, 1 min)
- Water and superplasticizer were added (low speed, 15 s)
- Mix everything (high speed, 1 min)
- Interrupt mixing process (1.5 min)
- Mix everything (high speed, 1 min)

After finishing the mixing process, consistency of the fresh mortar was determined and mixtures were moulded. From each mortar and consistency combination, ten prismatic specimens were made to determine the hardened properties of the mortar. On the one hand, four $25 \times 25 \times 285$ mm^3 prismatic specimens were made per mortar to measure free shrinkage according to EN 80112 under ambient laboratory conditions (20 °C, 60 R H.). Due to the consistency of the mortars, moulds were not vibrated but the surface had to be levelled. For 24 h after making the mix, specimens were demoulded and length of each specimen was measured at 1, 2, 7, 28, 56, 90, 128 and 180 curing days,

as shrinkage determines the maximum dimensions of the slab without shrinkage joints to prevent undesirable cracking. On the other hand, six $40 \times 40 \times 160$ mm^3 specimens were also made for each mortar to evaluate its hardened properties. As for the shrinkage specimens, moulds were not vibrated but the surface had to be levelled. For 24 h after making the mix, specimens were sealed and cured under ambient laboratory conditions and then, specimens were submerged in saturated lime water at 20±2 °C for another 28 days, as it is described in EN 12390.

2.2. Characterization of the hardened mortar

Physical, thermal and mechanical properties of the hardened mortar were determined in order to ensure that the mixes were suitable for radiant floor heating systems. All the tests but the shrinkage test were done on the same $40 \times 40 \times 160$ mm^3 specimens cured for 28 days according to the following sequence. First of all, dry bulk density (ρ) and water accessible porosity (n) were measured on each specimen in agreement with EN 1015-10. As the specimens must be oven dried during this procedure, the rest of the tests were done on oven-dried specimens. Then, thermal conductivity (λ) and volumetric heat capacity (c_v) of the hardened mortar were obtained with a HotDisk M1 tester, based on the Transient Plane Source (TPS) method developed by Gustafsson [31]. Test procedure is already explained in previous releases [32,33]. Final thermal conductivity and volumetric capacity of each mortar was obtained as the mean of 12 tests performed on the 6 specimens available. Ultrasonic Pulse Velocity (UPV) was later determined in order to estimate the quality of compaction of the hardened mortars. Ultrasonic direct tests were carried out by using a Proceq Pundit PL200 ultrasonic velocity tester. In this case, two 150 kHz piezoelectric transmitters were used to evaluate the mortar behaviour. Test was performed three times per specimen, for three different voltage-gain combinations: 100V-50X, 200V-50X and 400V-100X. The final UPV result for each specimen was the mean of the three values obtained. As the pulse must traverse the whole length of the specimen (L = 160 mm), UPV was determined based on the time (t) the pulse took from the emitter to the receiver ($UPV = L/t$). It is well known that porosity tends to decrease the UPV on hardened mortars, as the pulse velocity is significantly lower on air gaps than on either mortar paste or aggregates. Therefore, lower pulse velocities would be attributed to either a higher porosity or a less self-compactability. Anyway, both of them would negatively contribute to the thermal and mechanical performance of the mortars. Finally, mechanical properties of the hardened mortars were evaluated via flexural and compressive strength tests according to EN 1015-11 norm. Both tests were load controlled, with a load increment ratio of 50 N/s and 500 N/s for the flexural and compressive tests, respectively. As usual, specimens were tested first for flexural strength and then, the resulting halves were subjected to compressive tests. The representative values

Table 2
Mix proportions used on the study.

Mortar	Cement (C)	Lime Mud (LM)	Limestone Sand (L)	Super-plasticizer (SP)	Water (W)	Consistency			
						Before Shakes		After shakes	
[−]	[kg/m^3]	[kg/m^3]	[kg/m^3]	[kg/m^3]	[kg/m^3]	[mm]	[mm]	[mm]	[mm]
REF$_1$	544	0	1632	5.4	272	130	135	190	195
REF$_2$	537	0	1610	5.4	282	155	165	220	235
C10$_1$	502	56	1672	5.0	251	130	130	185	190
C10$_2$	495	55	1650	4.9	261	200	205	235	240
C20$_1$	445	111	1668	4.4	250	145	140	185	190
C20$_2$	439	110	1646	4.4	261	165	165	220	225
C30$_1$	388	166	1664	3.9	250	135	140	195	200
C30$_2$	384	165	1646	3.8	258	205	205	240	240
C40$_1$	332	221	1660	3.3	249	125	130	200	200
C40$_2$	329	219	1643	3.3	257	140	150	220	225

for each mortar were obtained as the mean of the 6 specimens for flexural strength, and as the mean of 12 halves for compressive strength.

2.3. Mortar performance on a radiant floor slab

In order to determine a more realistic value of the thermal performance of the mortars in a real system, a laboratory-scaled radiant floor heating system was built for the mortars chosen based on the previously obtained hardened mortar results. Fig. 2 shows the setup of the radiant floors studied, as well as the dimensions, thicknesses and thermal properties of all its constituents. Both 800 × 700 mm^2 radiant floor slabs made had expanded polystyrene as thermal insulation below, cross-linked polyethylene (PEX-a) pipes and the mortar to study in each case. A wire resistance introduced inside the water filled pipe provided uniform heating, which, being controlled by a thermostat, had a maximum heating power of 30W/m. Before every test, slabs were heated at 42 °C wire resistance constant temperature for at least 72 h to remove the excess of moisture associated with its construction process. After that, wire resistance was turned off and the system rested for 24 h to reach thermal equilibrium with the laboratory ambient temperature, 20 °C. The test itself had two different phases. On the first part, slab was heated until constant temperature was observed on the slab surface. Although both slabs took less than 10 h to reach stationary regime, both samples were heated for 10 h for practical reasons. During this time, temperature of the water inside the pipes was controlled and maintained by a thermostat at 42 °C. At the same time, mortar surface temperature was recorded every 5 min in the positions shown in Fig. 2a in

order to obtain a representative profile of the surface temperature of the heating system. Four tests were performed per mortar studied.

3. Results and discussion

3.1. Hardened mortar properties

To begin with, dry bulk density and water accessible porosity of the hardened mortars were evaluated. According to the results shown in Fig. 3, dry bulk density tended to decrease with the lime mud content, while the opposite was observed for the porosity. Lime mud decreased density by up to 2.6% and 3.6% for C40–1 and C20-2 mortars with respect to that of the REF$_1$ and REF$_2$ mortars, respectively. Porosity results were more consistent, presenting an increase of up to 27.5% and 36.1% for C40$_1$ and C40$_2$ mortars when compared with the same reference mortars. Regarding shrinkage, no significant differences were observed due to the lime mud addition, as all the mortars had a similar behaviour for both consistencies evaluated (see Fig. 4).

In order to have a qualitative estimation of the non-accessible porosity, UPV was also evaluated. As it is shown in Fig. 5, the higher the lime mud content, the lower it was the UPV. Reduction was more palpable for the most fluid consistencies, but the differences due to this property were not significant for a confidence interval of 95%. However, the reduction on UPV for C40$_1$ and C40$_2$ were up to 22.5% and 24% with respect to that of REF$_1$ and REF$_2$, respectively. In this case, differences were significant above 20% of cement replacement.
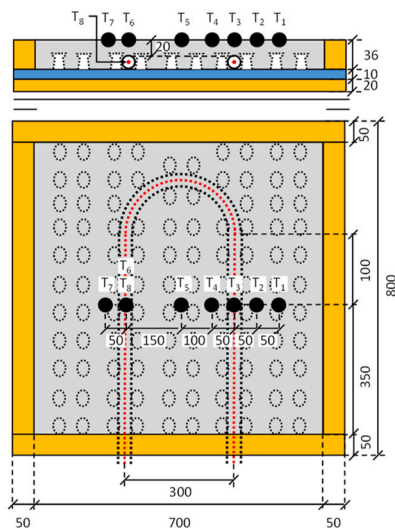
Colour	Material	Element (Size)	Thermal properties	
			λ [W/(mK)]	c_v [kJ/(m^{3}K)]
Grey	Mortar	Slab (800x700x36 mm^3)	It depends on the mortar studied.	
Black	Cross-linked Polyethylene	Piping (∅: 16 mm; t: 2 mm)	0.36	2187
Black	Polyethylene	Impervious, 3D layer (800x700x1 mm^3,)	0.46	1704
Blue	Expanded polystyrene	Bottom insulation (800x700x20 mm^3)	0.035	24
Amber	Glasswool	Bottom insulation (t: 50 mm)	0.035	30
Amber	Glasswool	Lateral insulation (t: 50 mm)	0.035	30

Fig. 2. Radiant floor system studied: a) General scheme: front and top views; b) slab ready to be tested, with the thermocouples on the slab surface; c) table including the dimensions and thermal properties of the materials used.
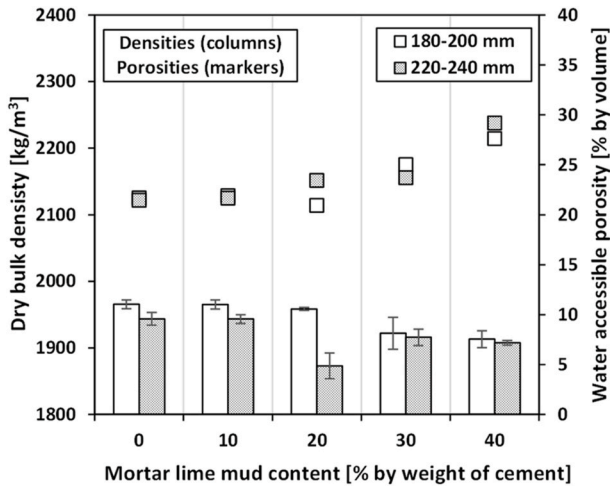
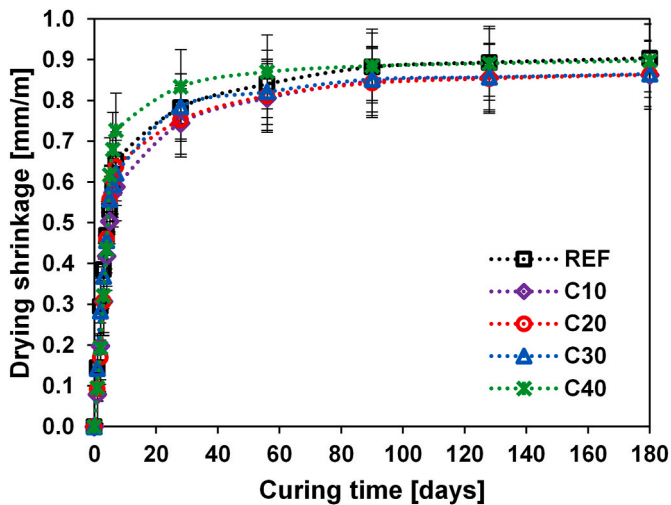**Fig. 3.** Effect of the lime mud proportion used on the mortar dry bulk density and porosity.

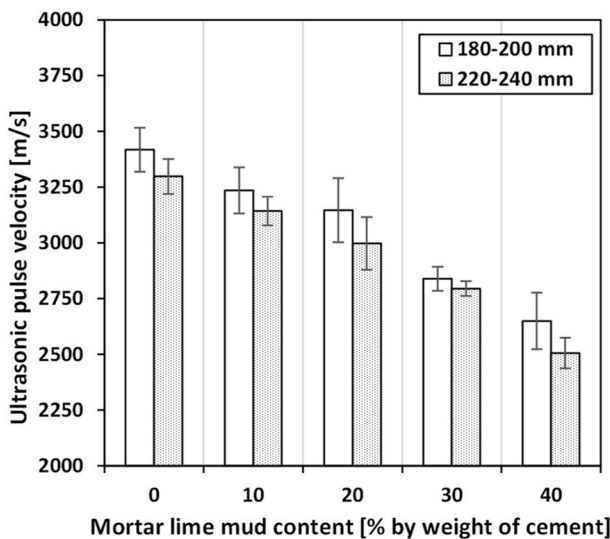**Fig. 4.** Shrinkage of the mortars as a function of the lime mud proportion used.

Fig. 5. Effect of the lime mud proportion used on the Ultrasonic Pulse Velocity of the hardened mortars.

In addition, Fig. 6 shows the thermal conductivity and the volumetric heat capacity of the mortar as a function of both the consistency and the lime mud proportion used. In general, the more fluid the consistency was, the lower the mortar thermal conductivity and the volumetric heat capacity were for the same lime content. Anyway, as for the UPV, differences between consistencies were not significant in most of the mortars evaluated. Regarding the influence of lime content, it caused a gradual thermal conductivity diminution of up to 8.1% ($C40_1$) and 15.5% ($C40_2$) for both consistencies. The effect of the lime content on the volumetric heat capacity of the resulting mortars was also similar to that observed for the thermal conductivity. The higher the lime mud proportions used, the lower it was the volumetric heat capacity of the material, with a maximum reduction of 10.5% and 23.8% on $C40_1$ and $C40_2$ mixes, respectively.

On stationary regime, mortar thermal performance mainly depends on the thermal conductivity of the material, while on transitory regime, thermal inertia also has a key role. Since radiant floors are designed for a continuous operation, most of the time radiant floors should be working on stationary regime. However, thermal inertia (I) should also be maximized in order to reduce the activation/deactivation cycles of the heating system. Thermal inertia of the mortar was determined by the well known equation (1):

$$I = \sqrt{\lambda \cdot c_v} \tag{1}$$

Thermal inertia for REF_1, $C10_1$, $C20_1$, $C30_1$ and $C40_1$ mixes were 1362 J/(m²s⁰·⁵K), 1316 J/(m²s⁰·⁵K), 1389 J/(m²s⁰·⁵K), 1323 J/(m²s⁰·⁵K) and 1236 J/(m²s⁰·⁵K), respectively, while that of the REF_2, $C10_2$, $C20_2$, $C30_2$ and $C40_2$ mixes were 1422 J/(m²s⁰·⁵K), 1375 J/(m²s⁰·⁵K), 1337 J/(m²s⁰·⁵K), 1272 J/(m²s⁰·⁵K) and 1141 J/(m²s⁰·⁵K), respectively. Hence, the reduction was more pronounced for the mortars with a more fluid consistency. In short, higher lime mud proportions and higher water quantities should decrease the time required by the system to reach stationary, but should also decrease its thermal efficiency when working stationary.

To finish the characterization of the hardened mortar, flexural and compressive strengths were determined (see Fig. 7). Regarding flexural strength, $C10_1$, $C20_1$, $C30_1$ and $C40_1$ mortars were 18%, 36%, 50% and 44% weaker than the REF_1 mortar, respectively. Likewise, $C10_2$, $C20_2$, $C30_2$ and $C40_2$ had a flexural strength 16%, 35%, 48% and 43% lower to that of the REF_2 mortar, in that order. In the same way, compressive strength of $C10_1$, $C20_1$, $C30_1$ and $C40_1$ mortars was 0.4%, 26%, 49% and 59% weaker to that of REF_1 mortar, while $C10_2$, $C20_2$, $C30_2$ and $C40_2$ mortars were 19%, 40%, 52% and 62% softer than their corre-
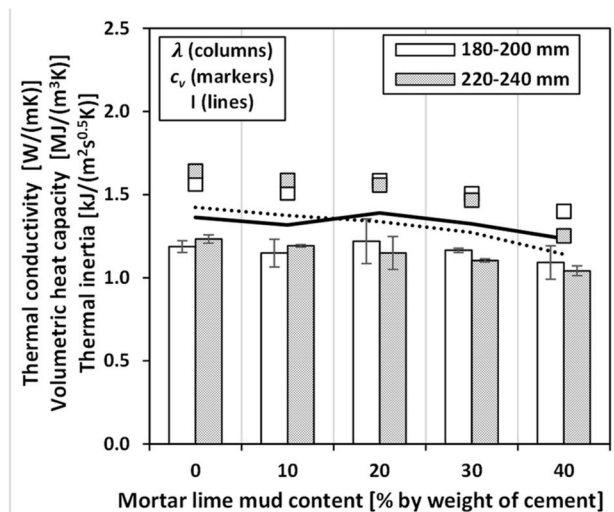

Fig. 6. Effect of lime mud proportion used on the thermal conductivity, volumetric heat capacity and thermal inertia of the hardened mortar.
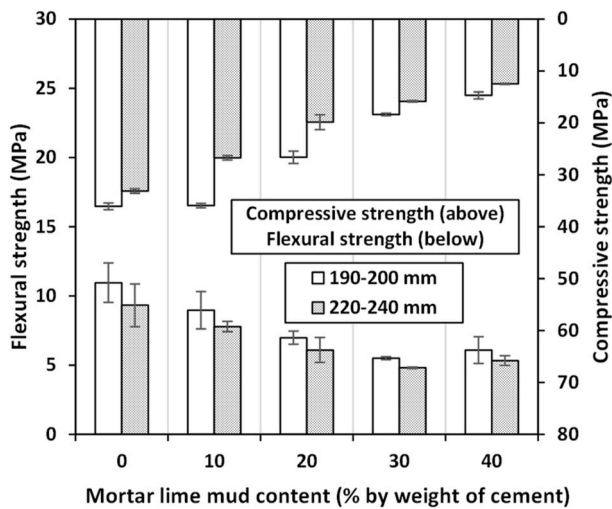
Fig. 7. Influence of the lime mud proportion used on the flexural and compressive strengths of the hardened mortar.

sponding REF$_2$ mortar. As lime mud had no hydraulic activity, it acted as an inert filler. Thus, replacing cement by lime mud led to mixes with higher aggregate to cement ratios (for example, 3 for the REF mortars, 5.67 for the C40 mortars). As the water required was almost the same as for the REF mortars for the required consistencies, water to cement of the mixes was increased leading to the weakening of the resulting hardened mortar [34].

As the lime mud used had no pozzolanic activity, cement was mainly replaced by a non-natural filler, which implied an increase in the water to cement *(W/C)* ratio. Fig. 8 shows the correlations of the hardened mortar properties with W/C ratio. Adding lime mud increased the W/C ratio of the mix, which increased the mortar porosity [20,23,25,35,36]. Due to the porosity increase, oven dried thermal conductivity was reduced, as its value for the air is lower than for the mortar cement paste or aggregates [37–40]. In fact, the higher porosity also eased the free-water release of the mortar during the drying process, reducing the volumetric heat capacity of the mortar. Higher porosity is also related to weaker flexural and compressive strengths [20,35,36,40] and lower UPVs [41–45]. Besides, those results are also in agreement with the results reported by Azevedo et al. [21,23] for a similar by-product, and clearly worse than the results obtained when the pozzolanity of this by-product is activated by calcination [19,25].

Hence, it is evident that the addition of lime mud had a negative effect on the thermal and mechanical properties of the mortar. However, mortars with up to 20% of lime mud cement replacement could be suitable for radiant floor heating applications, as the compressive strength of the C20$_1$ mortar, 27 MPa, was higher than the minimum of 20 MPa required by EN 1264-4:2010 standard. Furthermore, all the mortars studied could be used in other heat exchangers, such as Closed-Looped Geothermal Heat Exchanging systems, where there is no minimum mechanical strengths required as they do not have to be part of the structure.

3.2. Radiant floor performance

Based on the thermo-mechanical results obtained, Authors decided that C20$_2$ was the mortar that, having enough compressive strength, maximized the thermal performance. Thus, two different slabs were made in order to compare the real performance of C20$_2$ and REF$_2$ mortars. Fig. 9 shows two representative tests, one per each mortar studied.

In order to ease the comparison between both materials, maximum floor surface temperature increase (MFSTI) and difference between maximum and minimum surface temperature (DFST) were determined
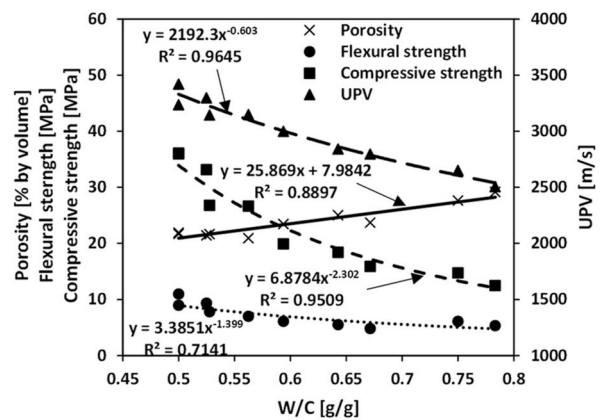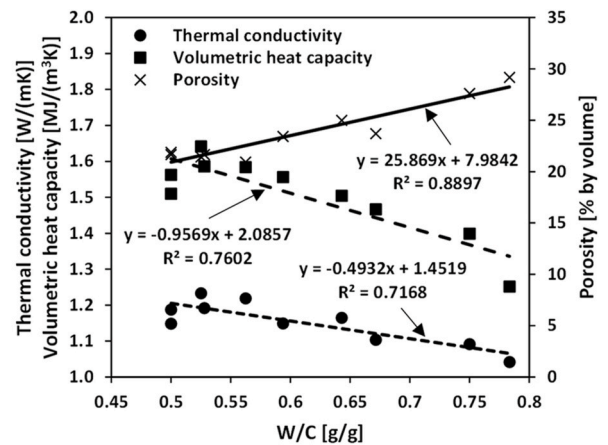

Fig. 8. Correlations of water to cement ratio, with the mortar hardened properties.

based on the variables proposed by Shin et at. [8], which resulted in equations (2) and (3):

$$MFSTI = \frac{50|\frac{T_2+T_3}{2}|+50|\frac{T_3+T_4}{2}|+50|\frac{T_6+T_7}{2}|}{150} - T_0 \quad (2)$$

$$DFST = MFSTI + T_0 - T_5 \quad (3)$$

where T$_0$ is the initial temperature of the system, 20 °C. As can be seen, the analysis was focused mainly in examining the temperature distribution between the pipes. According to the results shown in Fig. 10, MFSTI was 2.9% higher on the REF$_2$ slab to that of the C20$_2$ slab, thus the difference on thermal performance is insignificant, within a reasonable experimental confidence interval. However, for the DFST the difference is more pronounced, 12.9%, indicating that, for a similar thermal efficiency, C20$_2$ mortar had a more uniformly distributed surface temperature. Furthermore, MFSTI curves revealed that heating was also faster for the C20$_2$ slab, which is in agreement with the thermal inertia results obtained for each mortar.

4. Conclusions

This paper evaluates the influence of using lime mud, a by-product from the paper industry, as a partial replacement of cement on self-compacting mortars used in radiant floor heating systems. With that in mind, a reference mortar with cement: limestone sand weight proportions of 1:3, was compared to four different self compacting mortars, where cement was partially replaced by lime mud in four different proportions, 10%, 20%, 30% and 40%. After studying the physical, ther-
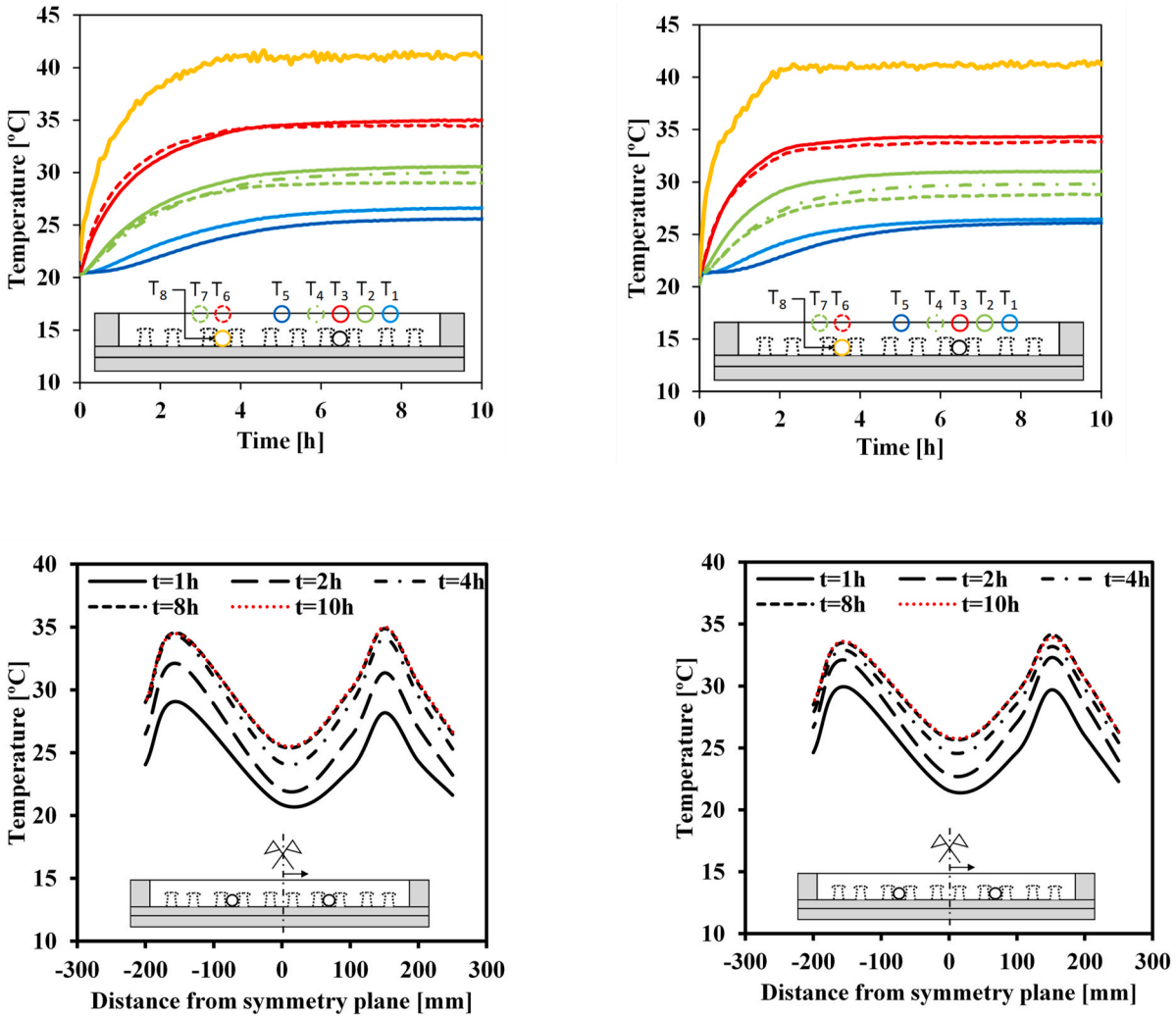
Fig. 9. Temperature evolution on different points of the slab during radiant floor heating tests: a) REF₂ slab; b) C20₂ slab.//Surface temperature profile at different times during radiant floor heating test: c) REF₂ slab; d) C20₂ slab.
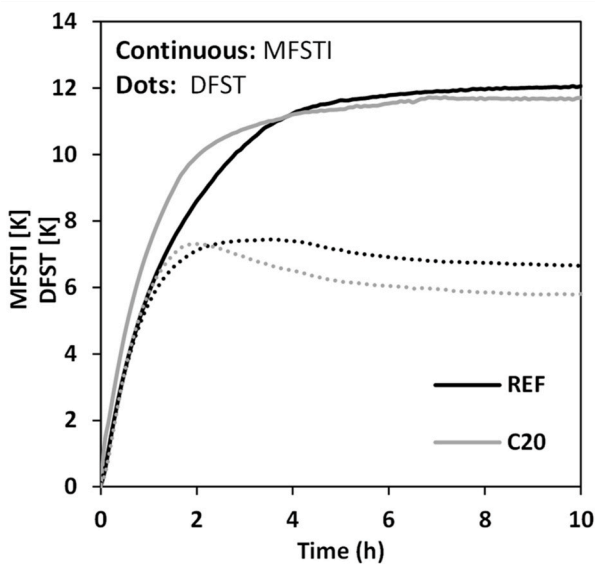

Fig. 10. Temperature evolution on the slab surface. Continuous lines: Average surface temperature increases. Dotted lines: Temperature dispersions on the surface.

mal and mechanical properties of the hardened mortar at an age of 28 days, Authors reached the following conclusions:

- The addition of lime mud decreased the thermal conductivity of the resulting mortar by up to 15% for the mortar with 40% of its cement replaced.
- The higher the lime mud used in the mix, the lower it was the volumetric heat capacity of the resulting mortars. Due to this reduction, thermal inertia of the mortars was reduced by up to 19% for the highest lime mud replacement ratio, 40%.
- Ultrasonic pulse velocity was reduced with the increase of the lime mud used, which is attributed to the higher porosity of the resulting mortars. Precisely, porosity increase caused by the higher water to cement ratio required is also responsible of the observed thermal conductivity and volumetric heat capacity reductions.
- Regarding mechanical properties, flexural and compressive strengths were reduced by up to 50% and 59%, respectively. However, replacement ratios of up to 20% could be used on most radiant floor systems, as the minimum compressive strength required, 20 MPa, is lower than the one obtained in those cases.
- Finally, two different slabs were made, one with the reference mortar, and the other with the mortar with 20% of cement replaced by lime mud. The average surface temperature increase was similar

in both cases. However, the surface temperature evenness was 12.9% better on the latter and its heating, faster.

Credit author statement

Roque Borinaga-Treviño: Conceptualization, Methodology, Investigation, Formal Analysis, Writing- Original Draft

Jesús Cuadrado Rojo: Methodology, Investigation, Visualization, Writing- Review & Editing

Javier Canales-Abaitua: Investigation, Writing- Review & Editing, Funding Acquisition

Eduardo Rojí Chandro: Methodology, Visualization, Writing- Review & Editing

Declaration of competing interest

The authors declare that they have no known competing financial interests or personal relationships that could have appeared to influence the work reported in this paper.

Acknowledgments

References

[1] M.- Yeo, I.- Yang, K.- Kim, Historical changes and recent energy saving potential of residential heating in Korea, Energy Build. 35 (2003) 715–727.
[2] Z. Zhuang, Y. Li, B. Chen, J. Guo, Chinese kang as a domestic heating system in rural northern China-A review, Energy Build. 41 (2009) 111–119.
[3] R. Bean, B.W. Olesen, K.W. Kim, History of radiant heating & cooling systems, ASHRAE J. 52 (2010) 40–47.
[4] R. Bean, B.W. Olesen, K.W. Kim, Part 2 history of radiant heating & cooling systems, ASHRAE J. 52 (2010) 50–55.
[5] K.- Rhee, B.W. Olesen, K.W. Kim, Ten questions about radiant heating and cooling systems, Build. Environ. 112 (2017) 367–381.
[6] C. Sebarchievici, D. Dan, I. Sarbu, Performance assessment of a ground-coupled heat pump for an office room heating using radiator or radiant floor heating systems, Procedia Eng 118 (2015) 88–100.
[7] L. Fontana, Numerical and experimental investigation on a concrete slab thermal conductivity increase due to metal cylinders perpendicular to the slab surface insertion, Appl. Therm. Eng. 120 (2017) 416–430.
[8] M.S. Shin, K.N. Rhee, S.R. Ryu, M.S. Yeo, K.W. Kim, Design of radiant floor heating panel in view of floor surface temperatures, Build. Environ. 92 (2015) 559–577.
[9] J. Kosny, A.D. Fontanini, N. Shukla, A. Fallahi, A. Watts, R. Trifu, et al., Thermal performance analysis of residential attics containing high performance aerogel-based radiant barriers, Energy Build. 158 (2018) 1036–1048.
[10] A.A.A. Abuelnuor, A.A.M. Omara, K.M. Saqr, I.H.I. Elhag, Improving indoor thermal comfort by using phase change materials: a review, Int. J. Energy Res. 42 (2018) 2084–2103.
[11] D. da Costa Reis, Y. Mack-Vergara, V.M. John, Material flow analysis and material use efficiency of Brazil's mortar and concrete supply chain, J. Ind. Ecol. 23 (2019) 1396–1409.
[12] M. Schneider, M. Romer, M. Tschudin, H. Bolio, Sustainable cement production-present and future, Cement Concr. Res. 41 (2011) 642–650.
[13] E. Benhelal, G. Zahedi, E. Shamsaei, A. Bahadori, Global strategies and potentials to curb CO2 emissions in cement industry, J. Clean. Prod. 51 (2013) 142–161.
[14] M.C.G. Juenger, R. Siddique, Recent advances in understanding the role of supplementary cementitious materials in concrete, Cement Concr. Res. 78 (2015) 71–80.
[15] J.K. Prusty, S.K. Patro, S.S. Basarkar, Concrete using agro-waste as fine aggregate for sustainable built environment – a review, Int J Sustain Environ 5 (2016) 312–333.
[16] M. Frías, R. Vigil De La Villa, R. García, M.I. Sánchez De Rojas, A. Juan Valdés, The influence of slate waste activation conditions on mineralogical changes and pozzolanic behavior, J. Am. Ceram. Soc. 96 (2013) 2276–2282.
[17] A. Gholizadeh Vayghan, A.R. Khaloo, F. Rajabipour, The effects of a hydrochloric
[18] F.F. Ataie, K.A. Riding, Thermochemical pretreatments for agricultural residue ash production for concrete, J. Mater. Civ. Eng. 25 (2013) 1703–1711.
[19] D. Ouyang, W. Xu, T.Y. Lo, J.F.C. Sham, Increasing mortar strength with the use of activated kaolin by-products from paper industry, Construct. Build. Mater. 25 (2011) 1537–1545.
[20] S. Yan, K. Sagoe-Crentsil, Properties of wastepaper sludge in geopolymer mortars for masonry applications, J. Environ. Manag. 112 (2012) 27–32.
[21] A.R.G. Azevedo, J. Alexandre, G.C. Xavier, E.B. Zanelato, M.T. Marvila, N.A. Cerqueira, et al., Study of durability of mortars with effluent sludge from paper industry exposed to salt spray, Miner Met Mater Ser (2018) 669–676 Part F8.
[22] M. Madrid, A. Orbe, H. Carré, Y. García, Thermal performance of sawdust and lime-mud concrete masonry units, Construct. Build. Mater. 169 (2018) 113–123.
[23] A.R.G. de Azevedo, J. Alexandre, G. Xavier, L.G. Pedroti, Recycling paper industry effluent sludge for use in mortars: a sustainability perspective, J. Clean. Prod. 192 (2018) 335–346.
[24] A.R.G. de Azevedo, J. Alexandre, M.T. Marvila, G.D.C. Xavier, S.N. Monteiro, L.G. Pedroti, Technological and environmental comparative of the processing of primary sludge waste from paper industry for mortar, J. Clean. Prod. 249 (2020).
[25] I. Vegas, J.J. Gaitero, J. Urreta, R. García, M. Frías, Aging and durability of ternary cements containing fly ash and activated paper sludge, Construct. Build. Mater. 52 (2014) 253–260.
[26] J. Malaiškienė, V. Banevičienė, R. Boris, V. Antonovič, The effect of dried paper-mill sludge on cement hydration, J. Therm. Anal. Calorim. 138 (2019) 4107–4118.
[27] R. Borinaga-Treviño, P. Pascual-Muñoz, D. Castro-Fresno, J.J. Del Coz-Díaz, Study of different grouting materials used in vertical geothermal closed-loop heat exchangers, Appl. Therm. Eng. 50 (2013) 159–167.
[28] R. Borinaga-Treviño, P. Pascual-Muñoz, M.Á. Calzada-Pérez, D. Castro-Fresno, Freeze-thaw durability of cement-based geothermal grouting materials, Construct. Build. Mater. 55 (2014) 390–397.
[29] R. Borinaga-Treviño, A. Orbe, J. Norambuena-Contreras, J. Canales, Effect of microwave heating damage on the electrical, thermal and mechanical properties of fibre-reinforced cement mortars, Construct. Build. Mater. 186 (2018) 31–41.
[30] R. Borinaga-Treviño, A. Orbe, J. Canales, J. Norambuena-Contreras, Experimental evaluation of cement mortars with recycled brass fibres from the electrical discharge machining process, Construct. Build. Mater. 246 (2020).
[31] S.E. Gustafsson, Transient plane source techniques for thermal conductivity and thermal diffusivity measurements of solid materials, Rev. Sci. Instrum. 62 (1991) 797–804.
[32] R. Borinaga-Treviño, A. Orbe, J. Canales, J. Norambuena-Contreras, Experimental evaluation of cement mortars with recycled brass fibres from the electrical discharge machining process, Construct. Build. Mater. 246 (2020).
[33] R. Borinaga-Treviño, A. Orbe, J. Norambuena-Contreras, J. Canales, Effect of microwave heating damage on the electrical, thermal and mechanical properties of fibre-reinforced cement mortars, Construct. Build. Mater. 186 (2018) 31–41.
[34] X. Chen, S. Wu, J. Zhou, Influence of porosity on compressive and tensile strength of cement mortar, Construct. Build. Mater. 40 (2013) 869–874.
[35] X. Chen, S. Wu, J. Zhou, Influence of porosity on compressive and tensile strength of cement mortar, Construct. Build. Mater. 40 (2013) 869–874.
[36] C.S. Poon, S.C. Kou, L. Lam, Compressive strength, chloride diffusivity and pore structure of high performance metakaolin and silica fume concrete, Construct. Build. Mater. 20 (2006) 858–865.
[37] R. Borinaga-Treviño, P. Pascual-Muñoz, D. Castro-Fresno, J.J. Del Coz-Díaz, Study of different grouting materials used in vertical geothermal closed-loop heat exchangers, Appl. Therm. Eng. 50 (2013) 159–167.
[38] K.- Kim, S.- Jeon, J.- Kim, S. Yang, An experimental study on thermal conductivity of concrete, Cement Concr. Res. 33 (2003) 363–371.
[39] W. Zhang, H. Min, X. Gu, Y. Xi, Y. Xing, Mesoscale model for thermal conductivity of concrete, Construct. Build. Mater. 98 (2015) 8–16.
[40] M. Baawain, H. Shoukry, K. Al-Jabri, An investigation into the thermo-physical, mechanical, and microstructural properties of cement mortar incorporating hybrid waste slags, Int. J. Civ. Eng. 19 (1) (2020) 17–26.
[41] Y. Ayaz, A.F. Kocamaz, M.B. Karakoç, Modeling of compressive strength and UPV of high-volume mineral-admixtured concrete using rule-based Mikt5 rule and tree model M5P classifiers, Construct. Build. Mater. 94 (2015) 235–240.
[42] T.U. Mohammed, M.N. Rahman, Effect of types of aggregate and sand-to-aggregate volume ratio on UPV in concrete, Construct. Build. Mater. 125 (2016) 832–841.
[43] M. Velay-Lizancos, I. Martinez-Lage, M. Azenha, P. Vázquez-Burgo, Influence of temperature in the evolution of compressive strength and in its correlations with UPV in eco-concretes with recycled materials, Construct. Build. Mater. 124 (2016) 276–286.
[44] K.R. Dabhekar, P.B. Nagarnaik, P.Y. Pawade, Relationship between compressive strength and UPV for concrete with partial replacement of GGBFS, Int. J. Civ. Eng. Technol. 8 (2017) 582–592.
[45] M.G. Hernández, M.A.G. Izquierdo, A. Ibáñez, J.J. Anaya, L.G. Ullate, Porosity estimation of concrete by ultrasonic NDE, Ultrasonics 38 (2000) 531–533.